Miniature Thermoluminescent Dosimeter Absorbed Dose Measurements in Tumor Phantom Models

Barry W. Wessels and M. Howard Griffith

Department of Radiology, The George Washington University, Washington, DC

Miniature teflon-imbedded $CaSO_4$:Dy thermoluminescent dosimeter(s) (TLD) have been sized and cut to fit inside a syringe needle. These dosimeters have been shown to be linear in response to beta and high energy gamma radiation. This allows for their direct implantation into tumor-bearing animals undergoing radioimmunotherapy and subsequent measurement of dose deposition on a per organ basis. In order to perform these radiolabeled antibody dose measurements with sufficient accuracy, static calibration data must first be generated. Consequently, phantom models were constructed with artificial tumors of diameters ranging from 3–30 mm contained in a surrounding tissue equivalent medium. The TLD were used to characterize dose distributions in a radial direction from the center of the cylindrical tumor volumes containing ^{131}I, ^{32}P, or ^{90}Y radionuclides. Absorbed dose measurements in the boundary region between tumor and outer medium were found to be dependent on the: (a) tumor specific activity, (b) average range of the beta radiation, and (c) radial tumor dimensions.

J Nucl Med 27:1308–1314, 1986

With the advent of tumor-associated monoclonal antibodies brought about by Kohler and Milstein's discovery of hybridoma technology in 1975 (*1*), diagnostic imaging for a variety of tumors using antibodies radiolabeled with either iodine-131 (^{131}I), iodine-123 (^{123}I), indium-111 (^{111}In), and perhaps technetium-99m appears to be a reality (*2–5*). An equal but somewhat less than optimistic view has been expressed in the feasibility of performing radioimmunotherapy with particulate radiation from radionuclides such as ^{131}I, yttrium-90 (^{90}Y), copper-67 (^{67}Cu), rhenium-186 (^{186}Re), astatine-211 (^{211}At) and others (*6–9*). Radioimmunotherapy modeling calculations based on MIRD type dosimetry (*10,11*) gives reasonable first-order estimates of gamma-emitting radionuclides in comparing the absorbed doses from organ to organ (S values) in humans, but fails to be predictive when examining particulate radiation in the subcentimeter range at tumor boundaries, for tumor heterogeneities, and at organ interfaces. In the MIRD formalism, particulate radiation is simply labeled "np" for nonpenetrating. Since it is envisioned that antibody therapy will be performed predominately by particulate radiation, heterogeneities in antibody deposition become a major factor in dose deposition and ultimately in the outcome of the tumor dose response to therapy. Consequently, substantial uncertainty in computing organ doses for radioimmunotherapy in animals or humans results from this method of dosimetry calculation which is highly dependent on basically unknown time dependent biodistribution data and internal organ geometry.

We have developed a method for the direct measurement of absorbed radiation dose through the use of teflon-imbedded, Teledyne $CaSO_4$:Dy thermoluminescent dosimeter(s) (TLD) which have been modified to fit inside a 20-gauge needle. Thermoluminescent dosimetry has been shown to be a reliable and accurate method of assessing radiation dose for a variety of health physics (*12*) and radiation therapy applications (*13*). As early as 1967, Kastner (*14*) recommended experimental animal biology based on Loevinger's formalism (*15*). It was shown that the light output from the thermoluminescent dosimeter is dependent only on the total absorbed energy and is not a function of specific ionization for high-energy beta and gamma radiation. This provides for a convenient dosimeter that may be calibrated for any internal beta emitter with a

Received Aug. 19, 1985; revision accepted Mar. 6, 1986.

For reprints contact: Barry W. Wessels, PhD, Div. of Radiation Oncology & Biophysics, The George Washington University Medical Center, 901 23rd St., N.W., Washington, DC 20037.

beta emission energy of at least 20 keV. These $CaSO_4$:Dy TLD were chosen over other available crystal types since they have been shown to be among the least energy dependent and the most sensitive when used in thickness which is substantially less than the radionuclide average beta range (*16*). The $CaSO_4$:Dy TLD may be directly implanted into a variety of animal or human organs in which dosimetric information is desired and subsequently recovered for read-out. In this work, we will discuss the fabrication and calibration of these dosimeters in a tumor phantom model and describe their relative accuracy and the reproducibility of dosimetry data for three radionuclides (^{131}I, phosphorus-32 (^{32}P), and ^{90}Y) which are of interest to the radioimmunotherapy community.

MATERIALS AND METHODS

The TLD used in the following phantom tumor model experiments were fabricated from 400-μ thick, 12-mm diameter $CaSO_4$:Dy teflon matrix disks*. Our experimental design required a sturdy, rod-shaped dosimeter that was designed to fit inside a syringe needle. Hence, we imbedded the disk dosimeter in a 2×2 cm^2 paraffin block for slicing the TLD with a tissue section microtome to a thickness of 200 μ. This TLD slab was then cut and accurately sized under a 20 power dissecting microscope to a length of 5 mm. The final dimensions of the dosimeter were $0.2 \times 0.4 \times 5.0$ mm^3. As shown in Fig. 1, the dosimeter conveniently fits inside a 20-gauge needle.

Each dosimeter was weighed (Mettler balance) and dimensions measured by micrometer to insure an initial overall uniformity of ±3%. These TLD were first cross calibrated with 4 MV x-rays from a Varian Clinac 4 linear accelerator at 20–1,500 cGy output under full buildup conditions (Fig. 2) as measured with a Farmer type ionization chamber. This ionization chamber calibration is traceable to the National Bureau of Standards. After reading under dry nitrogen, the TLD were reannealed (1 hr at 270°C) and counted for background light output. The TLD glow curve peak was integrated over 50 sec with $T_1 = 115$°C and $T_2 = 275$°C. Temperature ramping was 3.6°C/sec with prereadout annealing cycle of 5 sec. The major integration peak occurs at 220–240°C with a minor peak (5%) at 120°C for this material. In order to calibrate the dosimeters relative to a combined gamma and beta ray source, TLD rods were also immersed in a 5 ml, 1,020 μCi ^{131}I-NaI† water cylindrical phantom (d = 1 cm) for times ranging from 20 min to 24 hr (Fig. 3). A similar calibration experiment was performed with ^{90}Y in a 40-ml phantom over several hours (Fig. 4) and in a 25-ml ^{32}P phantom for a similar time period (Fig. 5). The dosimeters were kept in a fixed position and each was rinsed thoroughly with

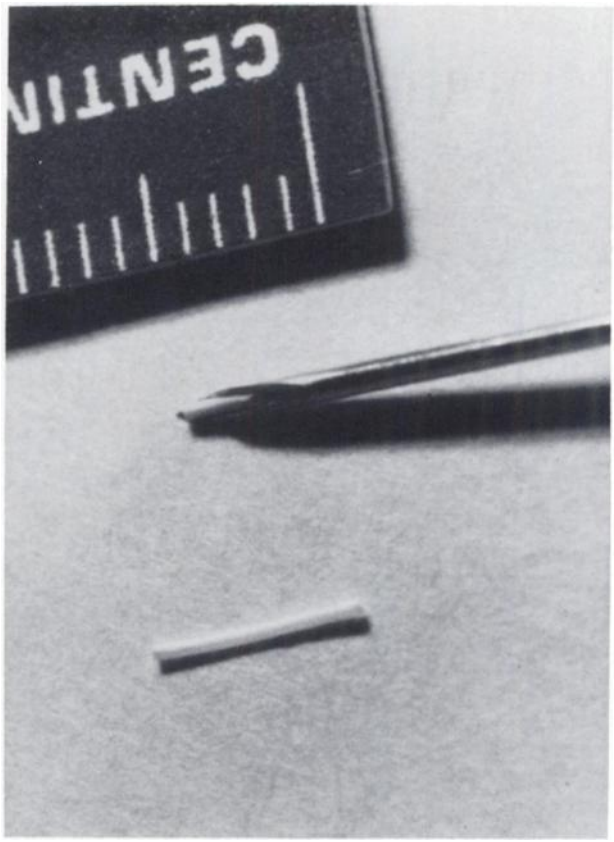

FIGURE 1
Tip of 20-gauge needle with miniature TLD in place for phantom implantation procedure. Second dosimeter is shown below needle for overall length comparison (5 mm)

Radiac wash upon removal from the solution. These TLD were read on the TLD reader in the same manner used for the 4 MV calibration experiment. Each data point was taken in threefold redundancy. No unusual TLD browning or discoloration due to exposure to the liquid suspension was noted after readout. The MIRD formalism was used in calculating the absorbed dose for these homogeneous, cylindrical phantoms in which the specific activities were known to ±5%. Resultant calibration factors of 0.99, 1.05, and 1.01 were calculated for ^{131}I, ^{90}Y, and ^{32}P relative to 4 MV x-ray radiation and were determined to an overall uncertainty of ±8%.

In addition, tumor phantom models were constructed from three different diameters of polystyrene test tubes or vials (Tube 1, d = 3.5 mm; Tube 2, d = 16 mm; and Tube 3, d = 30 mm) machined to uniform wall thickness of 0.3 mm in the region of TLD placement as shown in Fig. 6. Volumes of activity of tumor components were 0.8, 4.5, and 25 ml for tubes T_1, T_2, T_3, respectively. Inner tumor phantom components were placed in a larger outer box made of clear acrylic plastic of dimensions 10 cm × 10 cm × 15 cm^3 and filled with water to a volume of 900 ml.

For these experiments, each test tube tumor was

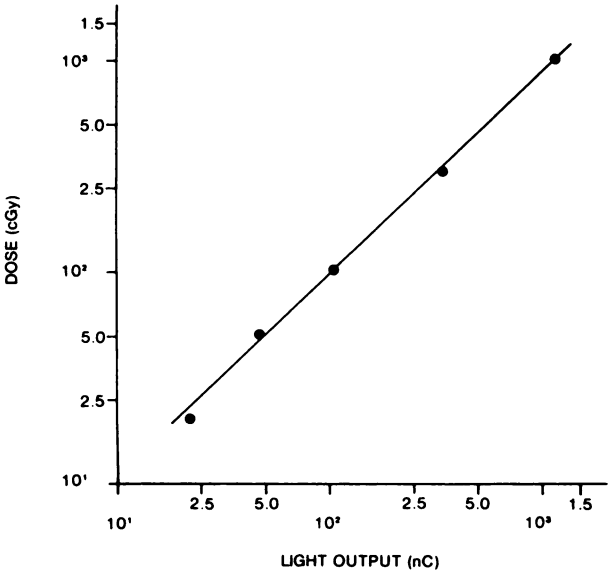

FIGURE 2
Log – log plot of TLD light output in nC of photomultiplier integrated charge collection vs. absorbed dose in cGy as measured by Farmer type chamber under full buildup and scatter conditions from 10 × 10 cm^2 4 MV isocentric 80 cm irradiation field in tissue equivalent Temex phantom. Each data point was taken in threefold redundancy. For these measurements, average conversion factor over dose range was 1 cGy = 1.13 ± 0.04 nC

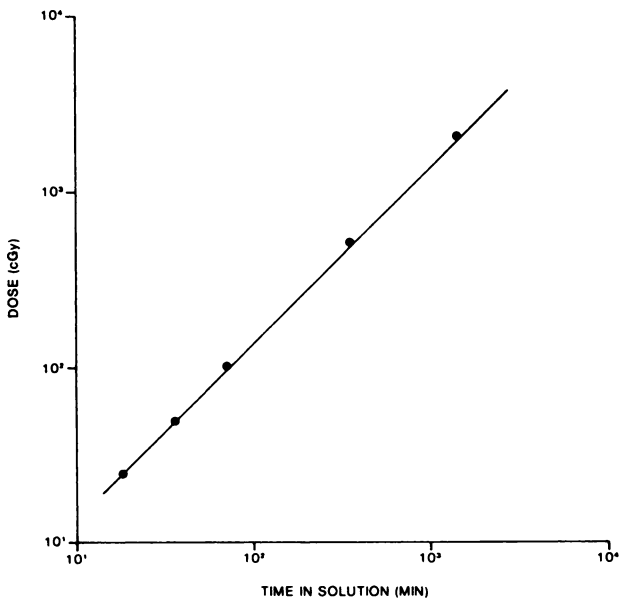

FIGURE 3
Log – log plot of absorbed dose in cGy vs. time in minutes of TLD fully immersed in a 1,020 μCi of ^{131}I 5 ml cylindrical water phantom. Carrier NaI (2 mg) was added to ensure homogeneous dispersion of ^{131}I-NaI. Decay corrected ^{131}I activities yield calibration factor of 1.12 ± 0.08 for cGy to nC TLD reader output based on MIRD calculations for this uniform geometry

placed midphantom in conjunction with the large outer box such that the central portion of the inner tumor was equidistant from the outer walls of the surrounding box. The inner test tube tumors were filled with activities of ^{131}I, ^{32}P, and ^{90}Y which were 10–200 times the specific concentration of activity relative to the outer phantom box. Activity measurements and manufacturer quotations were confirmed by gamma well or liquid scintillation counting methods as appropriate. Phosphorus-32 decay-corrected manufacturer's activity specifications were in agreement (±5%) with zero quenched serial diluted liquid scintillation counter reading (Beckman Model LS7500). Serial dilution volumes were 100-μl each, suspended in 10 ml of Scintiverse II scintillator cocktail. Yttrium-90 available privately‡ was calibrated by similar serial dilutions using the liquid scintillation counter. Scintillation counter values were used to determine activity in each of these experiments since the values showed ±20% variation from activities quoted by supplier. Knox gelatin was mixed with the water solution of activity (20 g/1,000 ml) before TLD implantation such that the resultant cooled media would physically stabilize the TLD position in the phantom.

The placement of the TLD was performed with the aid of an alignment jig and 20-gauge spinal needle (Fig. 6). The alignment jig was a machined 12 × 12 cm^2, 2-cm-thick lid which covered the top of the outer phantom. Forty holes were drilled and spaced from the center of the lid outward on a central line 1 mm apart. Each

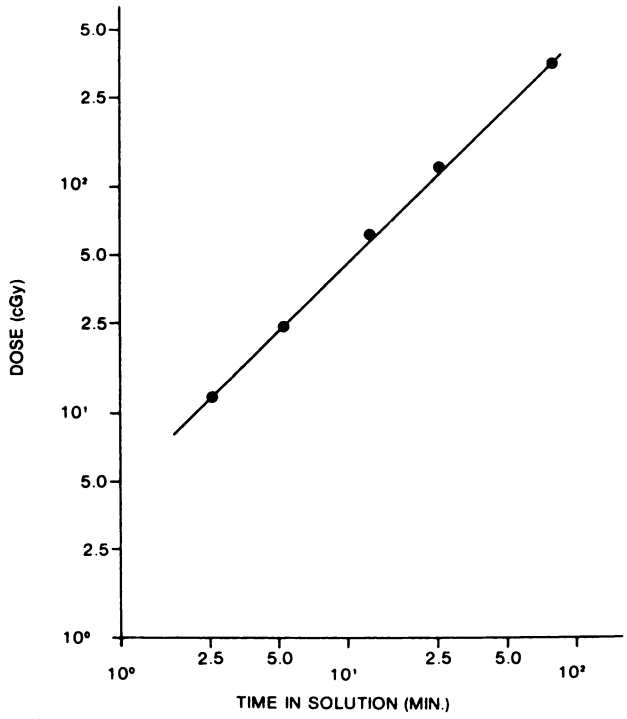

FIGURE 4
Log – log plot of absorbed dose in cGy vs. time in minutes of TLD fully immersed in 5,620 μCi of ^{90}Y-labeled protein 40 ml cylindrical phantom. Carrier protein (human serum albumin – 2 mg) was added to ensure homogeneous dispersion of ^{90}Y-labeled protein. Decay corrected ^{90}Y activities yield calibration factor of 1.19 ± 0.08 for cGy to nC TLD reader output based on MIRD calculations for this uniform geometry

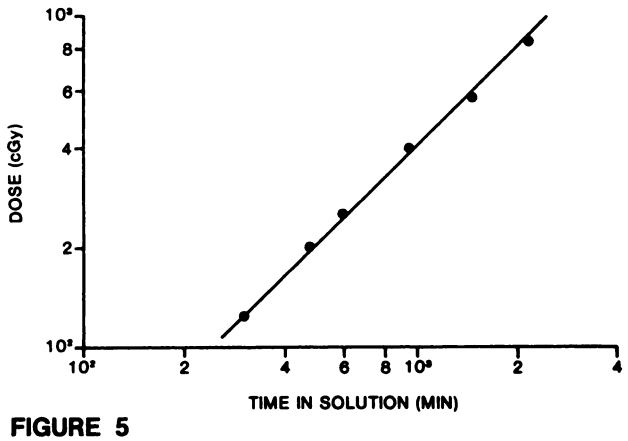

FIGURE 5
Log – log plot of absorbed dose in cGy vs. time in minutes of fully immersed TLD. Data were taken from three experiments which were conducted with a 25-ml cylindrical phantom containing 421 μCi of ^{32}P. Decay corrected ^{32}P activities yield calibration factor of 1.14 ± 0.08 for cGy to nC TLD reader output based on MIRD calculations for this uniform geometry

hole was oversize by 0.01 mm with the outer diameter of the 20-gauge spinal needle to facilitate tight sliding fit. The alignment jig afforded precise three-dimensional localization (±0.3 mm) of TLD radially outward from the center of the tumor to the wall region of the outer large phantom.

Between 10–15 TLD per experimental run were used to determine the dose profile in a radial direction for the tumor/outer phantom combination. TLD placement was over a range of radial distances starting at the inner tumor center and extending 4.5 cm outward. Nonuniform concentration of TLD placement was highest near the tumor wall and lowest in the regions greater than 1.5 cm from the inner tumor wall in order to characterize rapid dose variation near the interface region.

RESULTS

A total of nine phantom experiments were performed: three tumor sizes for each radionuclide, ^{131}I, ^{32}P, and ^{90}Y. For maximum utilization of these data without undue redundancy, results of these experiments are shown as plots of dose versus radial distance (Figs. 7–11). Each data point in these figures is the result of a single measurement with an associated standard error of ±15%. The calibration factors which were derived from the measurements described in the methods section were used to convert TLD light output (nC) to dose (cGy) for each radionuclide phantom experiment. Phosphorus-32 experiments are shown for all three tumor sizes in Figs. 7–9, and ^{131}I and ^{90}Y plots are

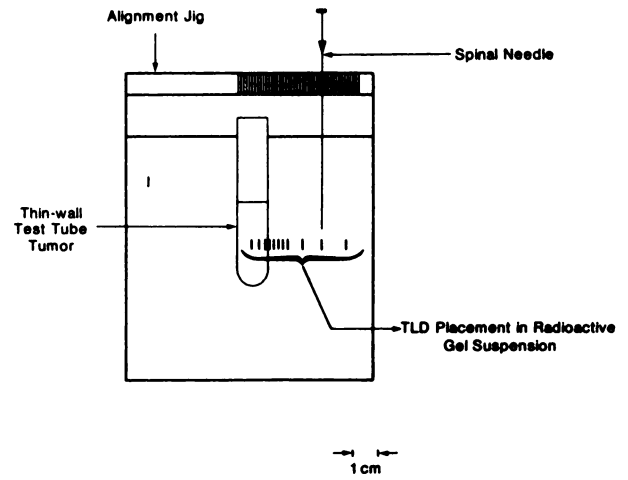

FIGURE 6
Tumor/normal tissue equivalent phantom. This is a thin-wall test-tube "tumor" imbedded in gel suspension of homogeneous radionuclide activity. Activity inside test tube is also in gel form ranging in specific activity 10–200 times that of specific activity of the outer media. TLDs are injected and suspended in gel for times ranging from 12–36 hr using alignment jig and spinal needle with inner stylus. All TLD are removed and recovered from gel simultaneously

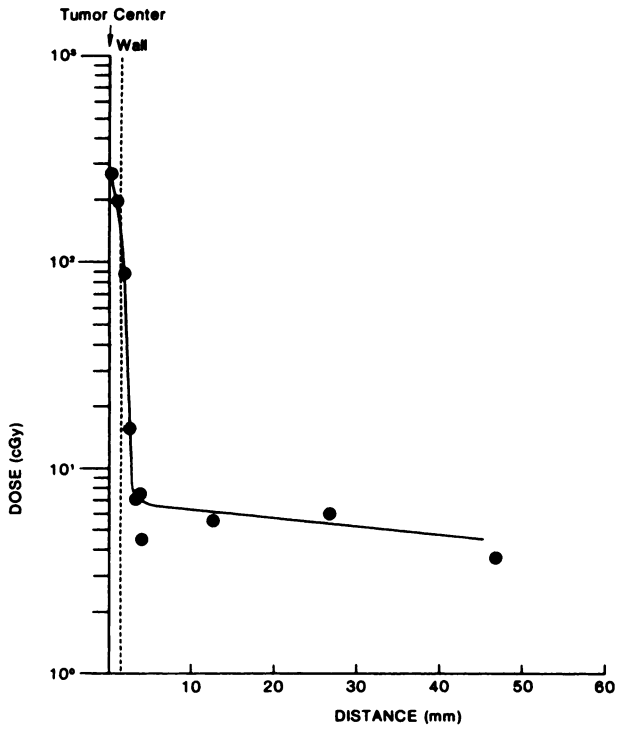

FIGURE 7
Dose measurements vs. distance from tumor center gel of TLD imbedded in tumor and outer phantoms containing ^{32}P in specific acitivity ratio of 73:1, respectively. Initial specific concentration of inner tumor was 22 μCi/ml. Total TLD suspension time was 16 hr. Half width measured from wall to 1/20th maximum peak height of curve drawn through data points is 0.7 ± 0.4 mm for tumor diameter of 3.5 mm

shown in Figs. 10 and 11, respectively, for test tube tumor number 3 only. Half-width, one-twentieth, or one-tenth maximum peak values (Γ_{20} or Γ_{10}) are given for each dose profile in order to characterize the effect of activity, range of particulate radiation, and tumor geometry. The half width of the curve is measured from the curve to the tumor wall. Quoted uncertainties associated with Γ were determined by graphic analysis using the single point data. A similar analysis is frequently used to characterize peak shapes obtained in nuclear spectroscopy studies (*17*). Curves were drawn as a best fit by visual examination.

DISCUSSION

By closely examining the data shown in Figs. 7–11, three immediate observations can be made with respect to dose deposition in and surrounding the tumor volume. First, specific activity or percent dose per g (volume) remains the first order or primary indicator of the magnitude of dose deposition. Secondly, beta particle range (R_{max} = 1.5, 8, 11 mm for ^{131}I, ^{32}P, and ^{90}Y, respectively) is the determinate factor to dose delivered near the tumor wall. The peak half-width, one-tenth maximum (Γ_{10}) for ^{131}I, ^{32}P, and ^{90}Y are 0.8 ± 0.5 mm (Fig. 10), 1.3 ± 0.5 mm (Fig. 9), and 2.5 ± 0.6 mm (Fig. 11), respectively, for the large tumor geometry (test tube number 3). It is important to note that these "effective dose ranges" are far below the quoted maximum ranges of the beta particles and are generally somewhat less than the average quoted beta ranges. This effect naturally leads into the third point of discussion: geometric size of the tumor. Examination of the ^{32}P data for different tumor data yields a Γ_{20} of 0.7 ± 0.4, 1.0 ± 0.4, and 2.0 ± 0.5 mm for progressively larger tumors, d = 3.5, 16, and 30 mm, respectively (Figs. 7–9).

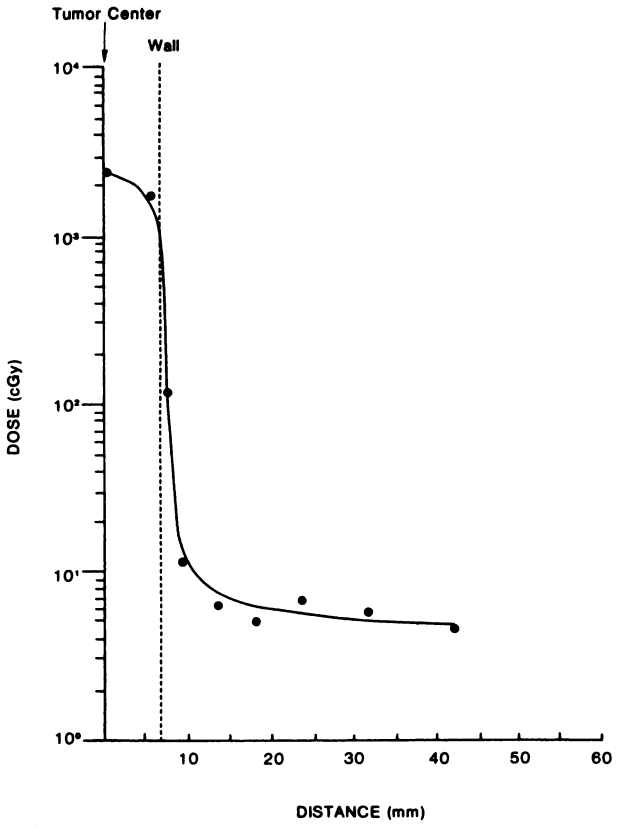

FIGURE 8
Dose measurements vs. distance from tumor center of TLD imbedded in gel tumor and outer phantoms containing ^{32}P in specific activity ratio of 200:1, respectively. Initial specific concentration of inner tumor was 80 μCi/ml. Total TLD suspension time was 16 hr. Half width measured from wall to 1/20th maximum of curve drawn through data points is 1.0 ± 0.4 mm for tumor diameter of 16 mm

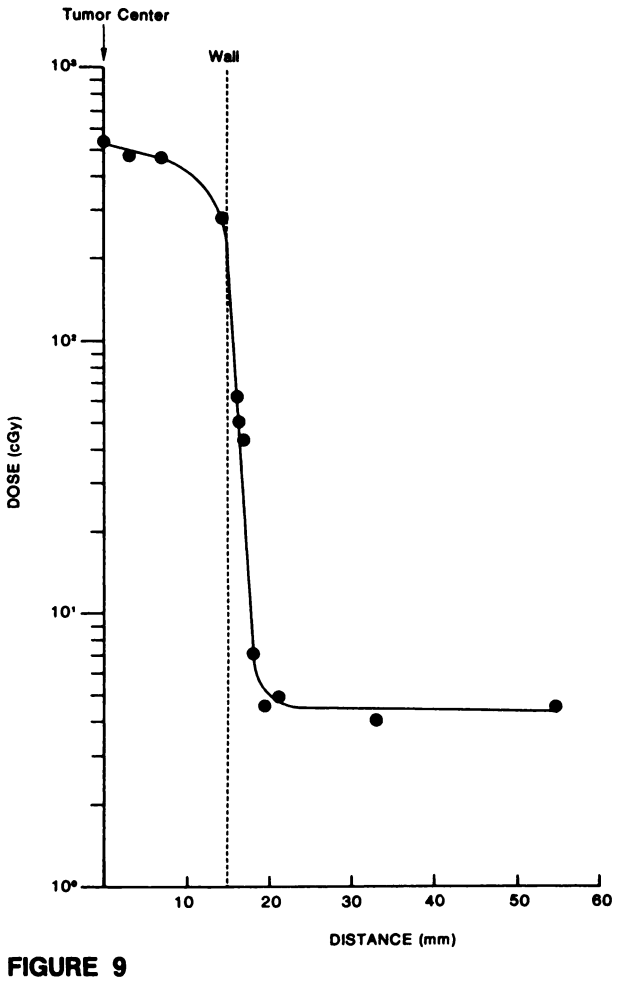

FIGURE 9
Dose measurements vs. distance from tumor center of TLD imbedded in gel tumor and outer phantoms containing ^{32}P in specific activity ratio of 89:1, respectively. Initial specific concentration of inner tumor was 21 μCi/ml. Total TLD suspension time was 18.5 hr. Half width measured from wall to 1/20th maximum of curve drawn through data points is 2.0 ± 0.5 mm for tumor diameter of 30 mm

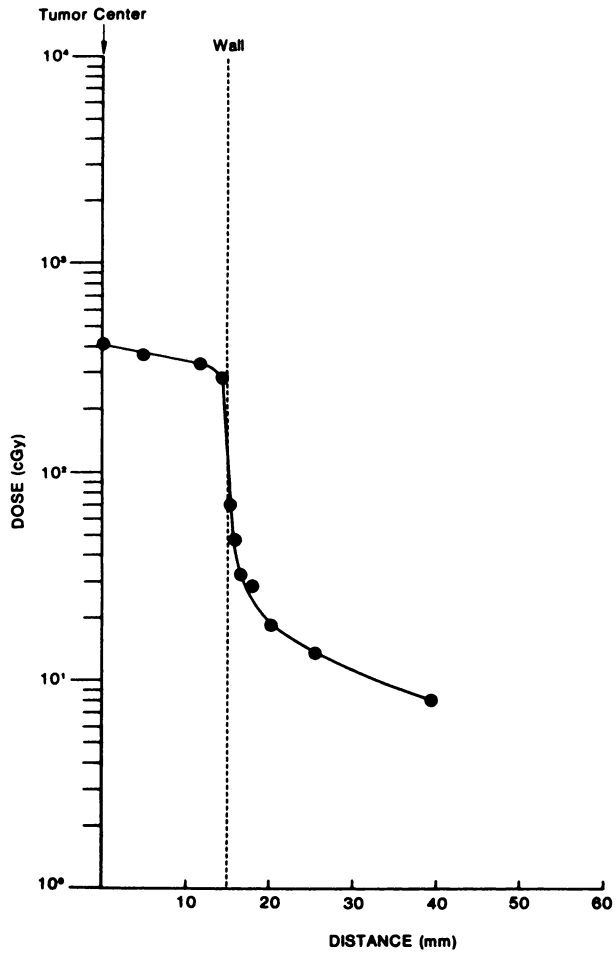

FIGURE 10
Dose measurements vs. distance from tumor center of TLD imbedded in gel tumor and outer phantoms containing ^{131}I in specific activity ratio of 70:1, respectively. Initial specific concentration of inner tumor was 72 μCi/ml. Total TLD suspension time was 20 hr. Half width measured from wall to 1/10th maximum of curve drawn through data points is 0.8 ± 0.5 mm for tumor diameter of 30 mm

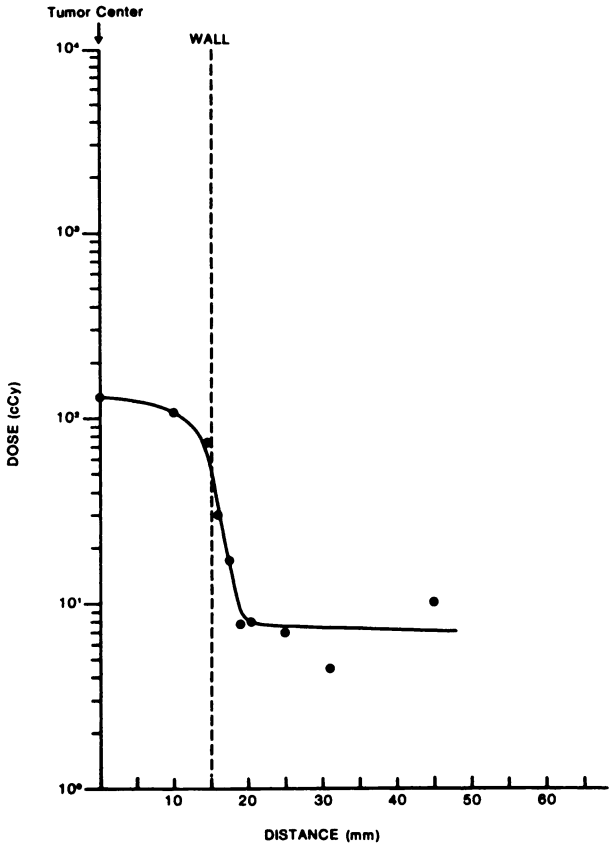

FIGURE 11
Dose measurements vs. distance from tumor center of TLD imbedded in gel tumor and outer phantoms containing ^{90}Y in specific activity ratio of 17:1, respectively. Estimated initial specific concentration of inner tumor was 6 μCi/ml based on post-calibration data with liquid scintillation counting and TLD comparison measurements. Total TLD suspension time was 12 hr. Half width measured from wall to 1/10th of curve drawn through data points is 2.5 ± 0.6 mm for maximum tumor diameter of 30 mm

The dose falloff region for these results appears to be similar to the idealized infinite sheet case calculated for ^{32}P as described by Leichner et al. (*18*). The overall tumor volume effect and beta range measurements here are also in reasonable agreement with calculations made by Kwok et al. (*19*) for spherical volumes. A subtler, but theoretically predicted, dose effect evident at the tumor boundary is that of the dose build-down in the region which occurs just inside the tumor boundary. The absorbed dose measured by the TLD in this region tends to decrease before the activity profile has started to decrease as shown in all doses vs. radial distance plots (Figs. 7–11).

The comparison of the linear accelerator calibration curve to the higher energy beta calibration data (^{90}Y, ^{32}P) shows good agreement with MIRD prediction for these simple geometries[§]. Although it has been reported that $CaSO_4$:Dy TLD exhibit an over response in sensitivity for low-energy x-ray irradiation (*20*), no correction was necessary to compensate for bremsstrahlung radiation produced from the beta emitters used in these experiments for the quoted accuracy of the measurements. Care must be exercised when applying these calibration methods to ^{125}I and ^{111}In radionuclides due to this over response in sensitivity for low-energy x-rays.

It is clear from the above boundary effect data that these direct measurements add a level of detailed description of dose profile at tumor/nontumor interfaces only obtained by complex point source functions or Monte Carlo techniques and are not readily accessible by the MIRD formalism. The presentation of the capabilities of these TLD as applied to activity interface problems for relatively simple phantom geometry has been aimed at providing a firm basis to more complex geometries encountered in vivo. Experiments are now

ongoing in which TLD dose information is being obtained from various organs and tumors in animals which are undergoing radioimmunotherapy with ^{131}I- or ^{90}Y-labeled tumor-associated monoclonal antibodies (*21*).

FOOTNOTES

* Teledyne, Inc., NJ.

† DuPont NEN Medical Products, No. Billerica, MA.

‡ Oak Ridge ^{90}Sr/^{90}Y generator, Hybritech Corp., La Jolla, CA.

§ For example, using the interval average decay-corrected activity (μCi) multiplied by time in hours or cumulated activity for the full buildup phantom shown in Fig. 9, the dose value for TLD absorbed dose may be computed by the expression

$$\frac{\tilde{A}_T}{M_T} \sum_i \Delta^i_{np}$$

for ^{32}P at the center of the tumor. Hence:

$$D_T = 20.8\ \mu Ci/g \cdot 18.5\ hr \cdot 1.48\ g \cdot rad/\mu Ci \cdot hr = 570\ rad.$$

This is to be compared with a TLD reading of 530 rad where 1 rad = 1 cGy. For other phantom experiments (Figs. 7–11), the tumor dose may be computed in a similar manner for full buildup conditions.

REFERENCES

1. Kohler G, Milstein C: Continuous cultures of fused cells secreting antibody of predefined specificity. *Nature* 256:495–497, 1975
2. Larson SM, Brown JP, Wright PW, et al: Imaging of melanoma with I-131-labeled monoclonal antibodies. *J Nucl Med* 24:123–129, 1983
3. Epenetos AA, Shepherd J, Britton KE, et al: Radioimmunodiagnosis of ovarian cancer using 123-I-labelled, tumor-associated monoclonal antibodies. *Cancer Detect Prevent* 7:45–49, 1984
4. Halpern SE, Hagan PL, Garver PR, et al: Stability, characterization, and kinetics of 111-In-labeled monoclonal antitumor antibodies in normal animals and nude mouse-human tumor models. *Cancer Res* 43:5347–5355, 1983
5. Paik CH, Saham MS, Hong JJ, et al: Preparation of a stable Tc-99m complex of (Fab')$_2$-DTPA and its biodistribution in mice. *J Nucl Med* 25:128, 1984
6. Goldenberg DM, Gaffar SA, Bennett SJ, et al: Experimental radioimmunotherapy of a xenografted human colonic tumor (GW-39) producing carcinoembryonic antigen. *Cancer Res* 41:4354–4360, 1981
7. Wessels BW, Rogus RP: Radionuclide selection and model absorbed dose calculations for radiolabeled tumor associated antibodies. *Med Phys* 11:638–645, 1984
8. DeNardo S, Erickson K, Benjamin E, et al: Monoclonal antibodies for radiation therapy of melanoma. *Proceedings of the Third World Congress of Nuclear Medicine and Biology*, Paris, Pergamon Press, 1982, pp 182–185
9. Quadri SN, Wessels BW, Dekazos D, et al: Radiolabeled biomolecules with Re-186: Potential for radioimmunotherapy. Symposium on Chemical Aspects of the Production and Use of Prospective Therapeutic Radionuclides, *ACS Abstracts*, Miami, FL, 1985
10. Loevinger R and Berman M: *A Revised Schema for Calculating the Absorbed Dose from Biologically Distributed Radionuclides, MIRD Pamphlet No 1, Revised*, New York, The Society of Nuclear Medicine, 1976
11. Snyder WS, Ford MR, Warner GG, et al: *"S", Absorbed Dose per Unit Accumulated Activity for Selected Radionuclides and Organs, MIRD Pamphlet No 11*, New York, The Society of Nuclear Medicine, 1975
12. *Thermoluminescent Dosimetry*, Cameron JR, Suntharalingam N, Kennedy GG, eds. Madison, WI, University of Wisconsin Press, 1968
13. *Applied Thermoluminescence Dosimetry*, Oberhofer M, Scharmann A, eds. Bristol, England, Adam Hilger, 1981
14. Kastner J, Hukko R, Oltman BG, et al: Thermoluminescent internal beta-ray dosimetry. *Rad Res* 32:625–640, 1967
15. Loevinger R, Japha EM, Brownell GL: Discrete radioisotope sources. In *Radiation Dosimetry*, Hine GJ, Brownell GL, eds. New York, Academic Press, 1956, pp 693–799
16. Piesch E: Application of TLD to personnel dosimetry. In *Applied Thermoluminescence Dosimetry*, Oberhofer M, Scharmann A, eds., Bristol, England, Adam Hilger, 1981, pp 167–195
17. Segre E: *Nuclei and Particles*, New York, W.A. Benjamin, 1965, pp 442–467
18. Leichner PK, Cash SA, Backx C, et al: Effects of injection volume on the tissue dose, dose rate, and therapeutic potential of intraperitoneal P-32. *Radiology* 141:193–199, 1981
19. Kwok CS, Prestwich WV, Wilson BC: Calculation of radiation doses for non-uniformly distributed beta and gamma radionuclides in soft tissue. *Med Phys* 12:405–412, 1985
20. Driscoll CMH: Fundamental aspects of TLD materials. In *Practical Aspects of Thermoluminescence Dosimetry*, CRS-43, London, England, The Hospital Physicists' Association, 1984, pp 5–11
21. Wessels BW, Bacha P, Quadri SN: Microdosimetric TLD measurements for tumor associated antibody therapy. *J Nucl Med* 25:39, 1984